

Supporting Information for:

A novel $\text{Sn}_2\text{Nb}_2\text{O}_7$ /defective carbon nitride heterojunction photocatalyst:
preparation and application for photocatalytic oxytetracycline removal.

Haoyu Zhang^a, Liman Peng^c, Huawei Li^d, Yiguo Su^{b*} and Shushu Huang^{a*}

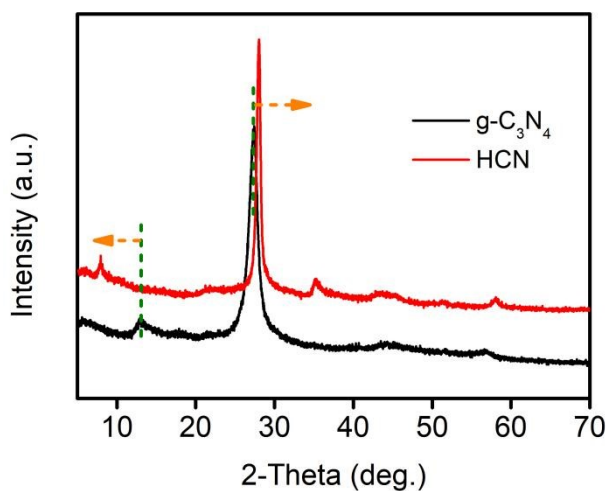
^aCollege of Light Industry and Textile, Inner Mongolia University of Technology,
Hohhot, 010080, China

^bCollege of Chemistry and Chemical Engineering, Inner Mongolia University, Hohhot,
Inner Mongolia 010021, P. R. China

^cTransportation Institute, Inner Mongolia University, Hohhot, Inner Mongolia
010021, P. R. China

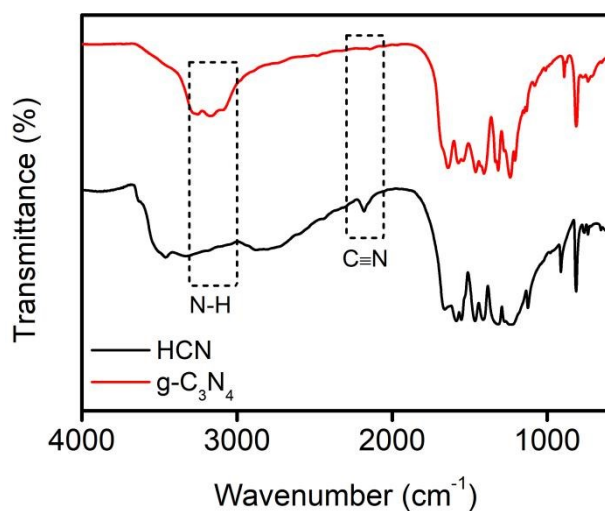
^dEcological Environment Monitoring and Monitoring Center Wuhai, Wuhai 016040,
China

Fig. S1 XRD patterns of g- C_3N_4 and HCN.



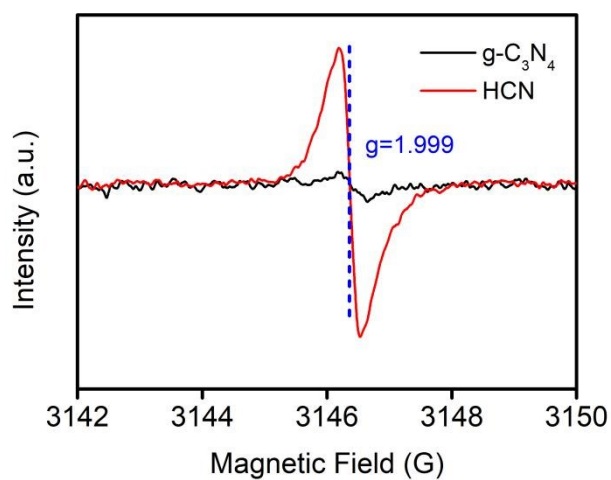
Clearly, it can be seen that the crystalline of HCN was improved after the modification of KSCN and acid. Meanwhile, the diffraction peaks of HCN shifted from 13.0° to 8.0° and 27.3° to 28.1° in comparison with g- C_3N_4 , indicating a larger in-plane arrangement distance and a compacted packing of heptazine layers.^{1,2}

Fig. S2 FT-IR spectra of g-C₃N₄ and HCN.



The additional peak appeared at 2180 cm⁻¹ in HCN can be related to the formation of -C≡N, deriving from the residual thiocyanogen groups.³ Meanwhile, the peak intensity of N-H in HCN sample weakened compared with g-C₃N₄, suggesting that the generation of -C≡N groups was from the deprotonation of NH_x group.⁴ Based on the above analysis, cyano- group was introduced in HCN, which could act as defective centers to boost the separation of photoinduced carriers.

Fig. S3 EPR spectra of g-C₃N₄ and HCN.



According to previous report, an EPR signal ($g = 1.999$) belonged to unpaired electrons on the sp^2 -carbon atoms of aromatic rings within π -bonded nanosized clusters, revealing the formation of nitrogen vacancies in carbon nitride.⁵ A higher EPR signal intensity of HCN was attributed to the introduction of cyano- groups, then accelerating the generation of unpaired electrons.

Fig. S4 TEM image of HCN (a) and $\text{Sn}_2\text{Nb}_2\text{O}_7$ (b).

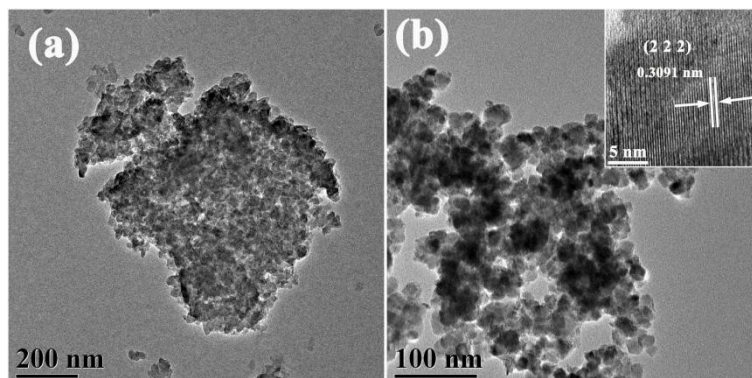


Fig. S5 Mott-Schottky plots of $\text{Sn}_2\text{Nb}_2\text{O}_7$ (a) and HCN (b).

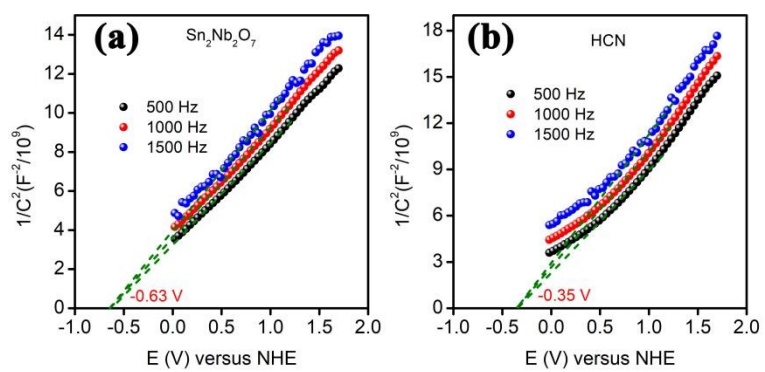
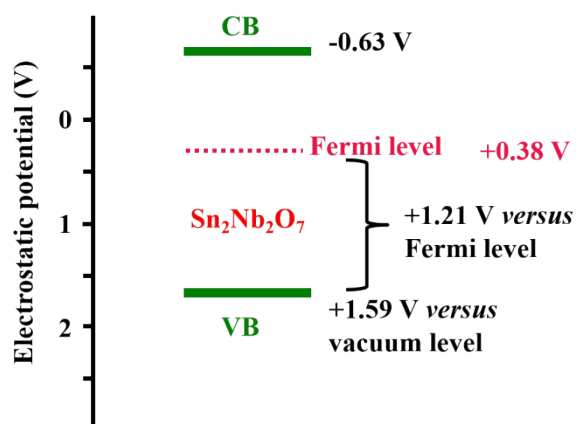


Fig. S6 Electronic structure of $\text{Sn}_2\text{Nb}_2\text{O}_7$.



The Fermi levels of $\text{Sn}_2\text{Nb}_2\text{O}_7$ and HCN were calculated by the results of VB-XPS and valence band energy results. As shown in Fig. S6, the VBM of $\text{Sn}_2\text{Nb}_2\text{O}_7$ versus vacuum level and Fermi level was 1.59 V and 1.21 V, respectively. The Fermi level of $\text{Sn}_2\text{Nb}_2\text{O}_7$ was calculated to be 0.38 V by subtracting the 1.21 V with 1.59 V. Similarly, the Fermi level of HCN was calculated to be 0.12 V.⁶

Fig. S7 The relationship between $\ln(C_0/C)$ and irradiation time for the degradation of OTC over all samples.

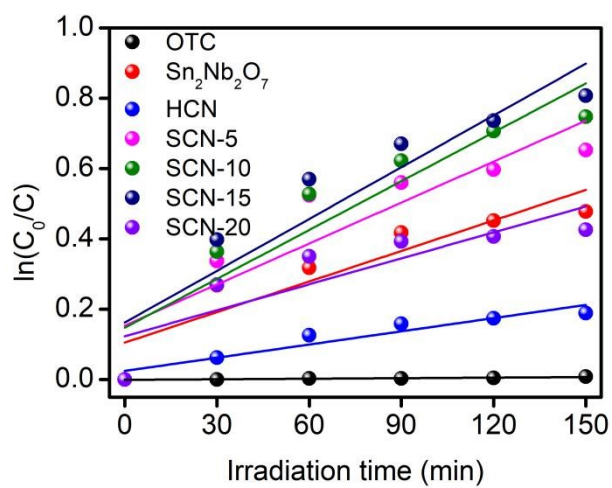
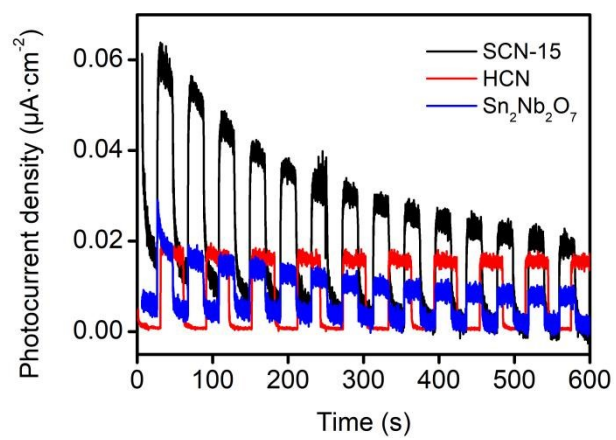


Fig. S8 Transient photocurrent response of samples.



References:

1. J. Yuan, Y. Tang, X. Yi, C. Liu, C. Li, Y. Zeng and S. Luo, *Appl. Catal. B: Environmental*, 2019, **251**, 206-212.
2. H. Li, B. Zhu, S. Cao and J. Yu, *Chem. Commun.*, 2020, **56**, 5641-5644.
3. H. Yu, R. Shi, Y. Zhao, T. Bian, Y. Zhao, C. Zhou, G.I.N. Waterhouse, L. Wu, C. Tung and T. Zhang, *Adv. Mater.*, 2017, **29**, 1605148.
4. J. Liu, Z. Wei, W. Fang, Z. Jiang and W. Shangguan, *ChemCatChem*, 2019, **11**, 6275-6281.
5. L. Yang, J. Huang, L. Shi, L. Cao, Q. Yu, Y. Jie, J. Fei, H. Ouyang and J. Ye, *Appl. Catal. B: Environmental*, 2017, **204**, 335-345.
6. J. Tang, R. Guo, W. Zhou, C. Huang, W. Pan, *Appl. Catal. B: Environmental*, 2018, **237**, 802-810.